J Mater Sci: Mater Med (2011) 22:2079–2088
DOI 10.1007/s10856-011-4379-3

Osteopenic bone cell response to strontium-substituted hydroxyapatite

E. Boanini · P. Torricelli · M. Fini · A. Bigi

Received: 27 April 2011 / Accepted: 9 June 2011 / Published online: 21 June 2011

Abstract Ionic substitution is a powerful tool to improve the biological performance of calcium phosphate based materials. In this work, we investigated the response of primary cultures of rat osteoblasts derived from osteopenic (O-OB) bone to strontium substituted hydroxyapatite (SrHA), and to hydroxyapatite (HA) as reference material, compared to normal (N-OB) bone cells. Strontium (Sr) and calcium (Ca) cumulative releases in physiological solution are in agreement with the greater solubility of SrHA than HA, whereas the differences between the two materials are levelled off in DMEM, which significantly reduced ion release. O-OB cells grown on SrHA exhibited higher proliferation and increased values of the differentiation parameters. In particular, Sr substitution increased the levels of proliferation, alkaline phosphatase, and collagen type I, and down-regulated the production of interleukin-6 of O-OB cells, demonstrating a promising future of SrHA in the treatment of bone lesions and defects in the presence of osteoporotic bone.

1 Introduction

There is an increasing interest in the improvement of biomaterials to replace diseased bone because of trauma, arthritis and tumors. Many patient-related conditions impair bone healing and remodeling and among these, osteoporosis is one of the most frequent diseases affecting bone cell proliferation, protein synthesis, cell reactivity to signal molecules and mesenchymal stem cell number [1]. Strategies based on bone grafting, biochemical (i.e., growth factors) and biophysical stimulation (i.e., pulsed electromagnetic fields and ultrasound), systemic administration or local release of antiresorptive and bone forming agents (i.e., bisphosphonates, parathyroid hormone) have been developed [2, 3]. Moreover, in order to avoid disease transmission risks and to have an unlimited supply of graft materials also avoiding donor site morbidity, different classes of bone substitutes such as hydroxyapatite, tricalcium phosphate, biological glasses, synthetic polymers, alone or in combination, are under investigation [2].

The composition of the mineral phase of bone is characterized by the presence of a number of foreign ions associated to the poorly crystalline carbonated apatite, which constitutes the inorganic component. Among these ions, Sr has received an increasing attention since the development and introduction of Sr ranelate in the treatment of patients with postmenopausal osteoporosis [4, 5]. Sr is reported to modify bone turnover in favor of bone formation and a mixed mode of action with increased bone formation and reduction of bone resorption has been suggested [6, 7]. As a matter of fact, Sr presence in bone is greater at the regions of high metabolic turnover, and in new than in old bone [8, 9]. The cellular action of Sr has been shown both in vivo and in vitro: it decreases bone resorption by inhibition of osteoclast resorbing activity and osteoclastic differentiation, and it promotes bone formation by enhancing pre-osteoblastic cell replication and osteoblastic differentiation [4, 10, 11]. The growing evidence of positive results obtained in clinical studies on strontium long-term treatment [6, 12] has stimulated a number of studies on Sr incorporation in biomaterials for bone tissue

E. Boanini · A. Bigi (✉)
Department of Chemistry "G. Ciamician",
University of Bologna, 40126 Bologna, Italy
e-mail: adriana.bigi@unibo.it

P. Torricelli · M. Fini
Laboratory of Preclinical and Surgical Studies, Research Institute Codivilla Putti, Rizzoli Orthopaedic Institute, Bologna, Italy

repair [13–17]. We have previously shown that Sr can influence cells response even when incorporated into hydroxyapatite (HA) structure. In particular, the results of the investigation carried out on Sr-substituted hydroxyapatite (SrHA) using osteoblast-like MG63 cells and human osteoclasts indicated that strontium influences bone cells behavior in a dose-dependent way. Sr concentrations in the range 3–7 at% significantly stimulate osteoblast activity and differentiation, whereas even 1 at%, Sr substitution is sufficient to affect osteoclast proliferation, which reduces on increasing Sr content [18]. Similar results were obtained on SrHA thin films deposited on titanium substrates by pulsed laser deposition, suggesting that the presence of Sr could not only enhance the positive effect of HA coatings on osteointegration and bone regeneration, but it also prevents undesirable bone resorption [14].

When cultured in vitro osteoblasts derived from aged or osteoporotic bone maintain some biological differences with respect to healthy bone derived cells both in basal conditions and, even more, when in direct contact with biomaterials [19–21]. This behavior is more representative of the clinical situation where the number of aged and osteoporotic patients affected by fragility fractures and other bone pathologies is increasing and the success rate of reconstructive surgery is lower than in healthy patients because of microarchitectural and biological bone alterations. By comparing results of experimental studies where the same biomaterials were tested in vitro in "pathological" and normal osteoblast cultures and implanted in bone of osteoporotic and normal animals, it was also demonstrated that in vitro models with osteoporotic bone derived cells turned out to be a predictor of the in vivo osteointegration rate [21, 22].

In order to provide a deeper insight into the role of Sr that is particularly aimed for osteoporotic patients, objective of the present study was the evaluation of the in vitro effect of SrHA on primary osteoblasts derived from osteopenic bone in comparison with healthy bone derived osteoblasts. For this purpose we used ovariectomized osteopenic rats and sham-aged as control, and comparatively studied morphology, viability, proliferation, extracellular matrix protein synthesis of osteoblasts cultured in direct contact with SrHA.

Moreover, we investigated the rate and amount of ionic release in physiological solution and in the cell medium, as well as the roughness of the materials, in order to provide a reliable interpretation of the in vitro results.

2 Materials and methods

2.1 Preparation and characterization of HA and SrHA

HA nanocrystals were synthesized in N_2 atmosphere as previously reported [23]: 50 ml of 1.08 M $Ca(NO_3)_2{\cdot}4H_2O$ solution at pH adjusted to 10 with NH_4OH was heated at 90°C and 50 ml of 0.65 M $(NH_4)_2HPO_4$ solution, pH 10 adjusted with NH_4OH, was added dropwise under stirring. The precipitate was maintained in contact with the reaction solution for 5 h at 90°C under stirring, then centrifuged at 10,000 rpm for 10 min and repeatedly washed with CO_2-free distilled water. The product was dried at 37°C overnight.

Sr containing HA was obtained following the same procedure but adding Sr^{2+} ions into the Ca^{2+} solution, before adjusting the pH to 10 with NH_4OH. To this purpose, the appropriate amounts of $Sr(NO_3)_2$ and $Ca(NO_3)_2{\cdot}4H_2O$ were dissolved in order to obtain a $[Sr/(Ca + Sr)] \times 100$ molar ratio of 10. The total concentration of $[Ca^{2+}] + [Sr^{2+}]$ was kept 1.08 M.

All chemical were purchased from Sigma-Aldrich Italia and used without further purification.

Ca and Sr contents in the solid products were determined by means of an inductively coupled plasma (ICP) mass spectrometer (ICP Optima 4200DV, Perkin Elmer). Powders were previously dissolved in 0.1 M HCl.

X-ray diffraction analysis was carried out by means of a PANalytical X'Pert PRO powder diffractometer equipped with a monochromator in the diffracted beam. CuKα radiation was used (40 mA, 40 kV). The 2θ range was from 10° to 60° at a scanning speed of 0.75°/min. In order to evaluate the coherence lengths of the crystals and the apatitic lattice parameters, further X-ray powder data were collected in the 2θ range from 10° to 60° in step scanning mode with a fixed counting time of 10 s for each 0.030°/step.

Disk-shaped samples, diameter = 13 mm, were prepared by pressing 300 mg of powders into cylindrical moulds.

For Atomic Force Microscopy (AFM) imaging a Veeco Nanoscope 3D instrument was used. The disk-shaped samples were analyzed in tapping mode using a E scanner (maximum scan size 15 μm) and phosphorus(n)-doped silicon probes (spring constant 20–80 N/m; resonance frequency 250–290 kHz; nominal tip radius <10 nm). Roughness parameters, namely arithmetic mean roughness (Ra), root-square roughness (Rq), and the vertical distance between the highest and lowest points within the evaluation length (Rmax), were recorded on three samples of HA and on three samples of SrHA.

Release of Ca and Sr from disk-shaped samples in physiological solution (NaCl 0.9%) and in DMEM was measured up to 14 days by an ICP spectrometer (ICP Optima 4200DV, Perkin Elmer). The volume of the release solution utilized for each disk-shaped sample (300 mg) was 1 ml. Results from this analysis represent the mean value of three different determinations.

Energy dispersive X-ray spectrometry (EDS) analyses were performed on disk-shaped samples before and after

release in physiological solution using a Philips XL-20 microscope.

Before cell experiments, the disks were sterilized with gamma rays (Cobalt-60) at a dose of 25 kGy.

2.2 Cell culture and analyses

2.2.1 Osteoblast isolation and culture

Rat osteoblasts were sterilely isolated from small specimens derived from the trabecular bone of the distal femurs of Sprague–Dawley normal or osteoporotic female rats, aged 13 months. Estrogen-deficient osteoporosis was obtained 3 months after bilateral ovariectomy in 10 month-old rats, as a well characterized model by means of densitometric, ultrasonographic, mechanical and histomorphometric analyses [24]. All animals were used, handled, maintained and euthanized by strictly following International and European Laws on animal experimentation and after local Ethic Committee approval. In aseptic conditions, the distal femurs were cleaned from soft tissues and the cortical area was removed with a bone cutter in order to expose the trabecular tissue used for osteoblast cultures. Trabecular bone fragments from distal femurs were put in DMEM:F12 (Sigma, UK) serum-free culture medium and immediately processed to obtain primary cultured osteoblasts. Bone fragments were repeatedly washed with DMEM:F12 serum-free medium, and digested in medium with 1 mg/ml collagenase (Sigma) for 90 min at 37°C. The enzymatic reaction was stopped by adding an equal volume of medium with 10% of FCS and the supernatant containing the released cells was collected. Washing and collecting were repeated three times. The cells obtained were pelletted by centrifugation, resuspended, seeded in culture flasks (75 cm^2), and cultured in DMEM medium containing 10% FCS (Lonza CH), and 1% antibiotics (Penicillin 100 U/ml, Streptomycin 100 µg/ml, Invitrogen, USA), and incubated at 37°C in a humidified 95% air/5% CO_2 atmosphere.

At 90% confluence, cells were detached from culture flasks by trypsinization, and centrifuged; cell number and viability were checked with trypan blue dye exclusion test.

Osteoblasts derived from both normal (N-OB) and osteopenic (O-OB) bone were plated at a density of 2×10^4 cells/ml in 24-well plates containing six sterile samples each (∅ 13 mm) of HA and SrHA, obtaining the following experimental groups: N-HA, N-SrHA, O-HA, O-SrHA. The same concentration of cells was seeded in empty wells for control of experiment (N-OB, O-OB). Medium was changed with DMEM additioned with β-Glycerophosphate (10 mM, Sigma) and Ascorbic acid (50 µg/ml, Sigma) to activate osteoblasts, and plates were cultured in standard conditions, at 37°C ± 0.5 with 95% humidity and 5% CO_2 ± 0.2 up to 14 days. For the production of osteocalcin the culture medium was enriched with $1.25(OH)_2D_3$ (10^{-9}M, Sigma) 48 h before end of each experimental time (7 and 14 days).

2.2.2 Osteoblast proliferation

Cell proliferation and viability (3, 7, and 14 days) was monitored by WST1 (WST1, Roche Diagnostics GmbH, Manheim, Germany) colorimetric reagent test. The assay is based on the reduction of tetrazolium salt to a soluble formazan salt by a reductase of the mitochondrial respiratory chain, active only in viable cells. 50 µl of WST1 solution and 450 µl of medium (final dilution: 1:10) were added to the cell monolayer, and the multi-well plates were incubated at 37°C for a further 4 h. Supernatants were quantified spectrophotometrically at 450 nm with a reference wavelength of 625 nm. Results of WST1 are reported as optical density (OD) and directly correlate with the cell number.

2.2.3 Osteoblast activity and differentiation

At the end of experimental times (7 and 14 days) the supernatant was collected from all wells and centrifuged to remove particulates, if any. Aliquots were dispensed in Eppendorf tubes for storage at −70°C and assayed for Bone Alkaline Phosphatase activity (BAP, immunoassay kit, USCN Life Science, Wuhan, China), Type I Pro-Collagen (PC I, immunoassay kit, USCN Life Science, Wuhan, China), Osteocalcin (OC, immunoassay kit, Biomedical Technologies, MA, USA), Interleukin-6, (IL-6, immunoassay kit, Bender Medsystems, A), and Tumor Necrosis Factor-α (TNF-α, immunoassay kit, Diaclone, F); all kits were specific for rat. All the measured concentration and activity were normalized by Total Protein content (TP, Total Protein micro-Lowry kit, SIGMA, MO, USA) at 7, and 14 days, to take into account the differences in cell growth.

2.2.4 Cell morphology

Samples for each material, at the end of the experiment, were processed for scanning electron microscopy (SEM): osteoblasts grown on the materials were fixed in 2.5% glutaraldehyde, in pH 7.4 phosphate buffer 0.01 M for 1 h and dehydrated in a graded ethanol series. After a passage in hexamethyldisilazane, the samples were air dried. Samples were sputter-coated with Pd before examination with a Philips XL-20 SEM operating at 10 kV.

2.2.5 Statistical analysis

Statistical evaluation of data was performed using the software package SPSS/PC$^+$ Statistics^{TM} 10.1 (SPSS Inc.,

Chicago, IL, USA). The experiment was repeated 3 times and the results presented are the mean of six samples each. Data are reported as mean ± standard deviations (SD) at a significance level of $P < 0.05$. After having verified normal distribution and homogeneity of variance, a one-way ANOVA was done for comparison between groups. Finally, the Scheffé's post hoc multiple comparison tests were performed to detect significant differences between groups.

3 Results and discussion

The powder X-ray diffraction patterns of the as-synthesized products confirm that they are constituted of HA as unique crystalline phase [23]. The cell parameters of the sample synthesized in presence of Sr are slightly enlarged with respect to those of the sample obtained in the absence of Sr, as reported in Table 1. The enlargement of the unit cell provoked by the partial replacement of Ca^{2+} (ionic radius 0.099 nm) with the bigger Sr^{2+} (ionic radius 0.12 nm) is in agreement with the amount of Sr incorporated into the nanocrystals, which accounts for 9.8 ± 0.3 at% (mean value of the measurements performed on five samples). Figure 1 reports the comparison between the powder X-ray diffraction patterns of HA and of SrHA in two selected ranges of 2θ: 24–27° and 38–41°, where the 002 and 310 reflections are centred, respectively. In agreement with the greater cell parameters of SrHA, both the reflections appear shifted to smaller angles in the pattern from SrHA (b) with respect to that of HA (a). Moreover, the reflections of SrHA appear broader than those of HA, indicating shorter lengths (τ_{hkl}) of the perfect crystalline domains. τ_{hkl} values, which are related to the crystal size and strain in the long dimension (002) and the cross section (310) of the apatite crystals, were calculated from the full width at half maximum intensity (FWHM) using the Scherrer equation [25]:

$$\tau_{hkl} = \frac{k\lambda}{FWHM \cos\theta} \quad (1)$$

where λ is the wavelength, θ the diffraction angle and K a constant depending on crystal habit (chosen as 0.9). The values of τ_{hkl} reported in Table 1 indicate that Sr substitution for Ca provokes a significant reduction of the coherent length both along the direction parallel to the

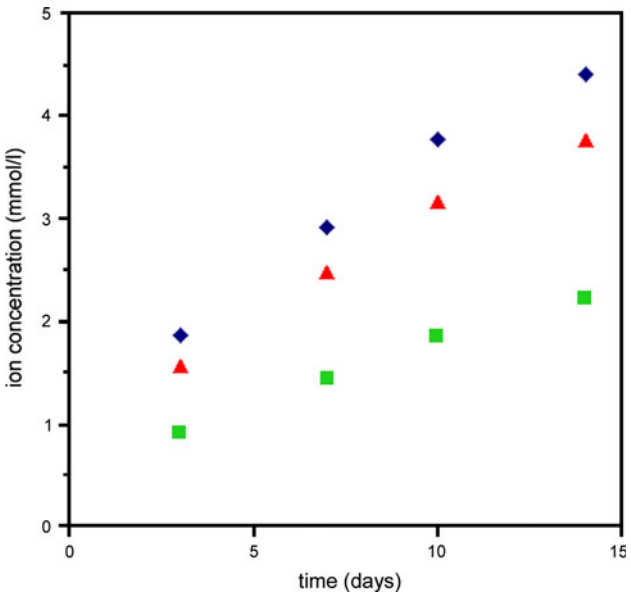

Fig. 2 Calcium and Strontium cumulative release from HA and SrHA as a function of soaking time in physiological solution. Ca from HA (*filled diamond*); Ca from SrHA (*filled square*); Sr from SrHA (*filled triangle*)

Table 1 Lengths (τ_{hkl}) of the perfect crystalline domains calculated using the Scherrer method, and cell parameters of SrHA and HA

Sample	τ_{002} (Å)	τ_{310} (Å)	*a*-axis (Å)	*c*-axis (Å)
HA	469 (5)	224 (6)	9.4269 (3)	6.8840 (2)
SrHA	319 (7)	150 (3)	9.457 (1)	6.9158 (6)

Each value is the mean of the measurements performed on five samples, and it is reported with its standard deviation

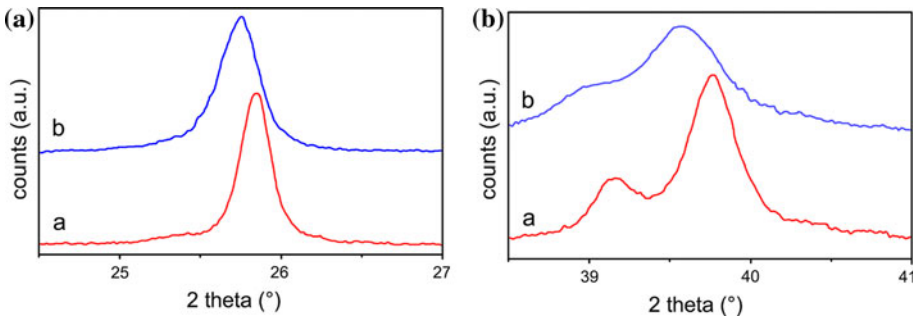

Fig. 1 Powder X-ray diffraction patterns of HA (**a**) and of SrHA (**b**) in two selected ranges of 2θ°

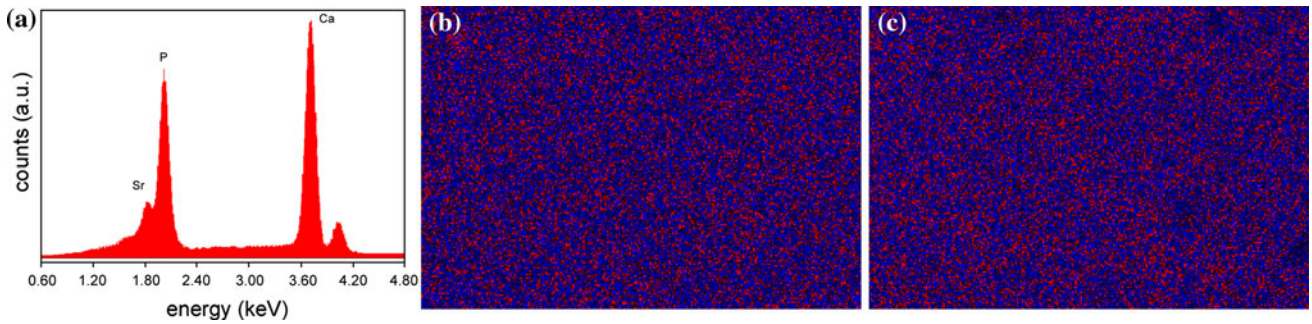

Fig. 3 **a** EDS spectrum of a SrHA disk-shaped sample. EDS maps recorded from SrHA disk-shaped sample before (**b**) and after (**c**) immersion in physiological solution for 14 days. Ca is *black/blue*; Sr is *grey/red* (Color figure online)

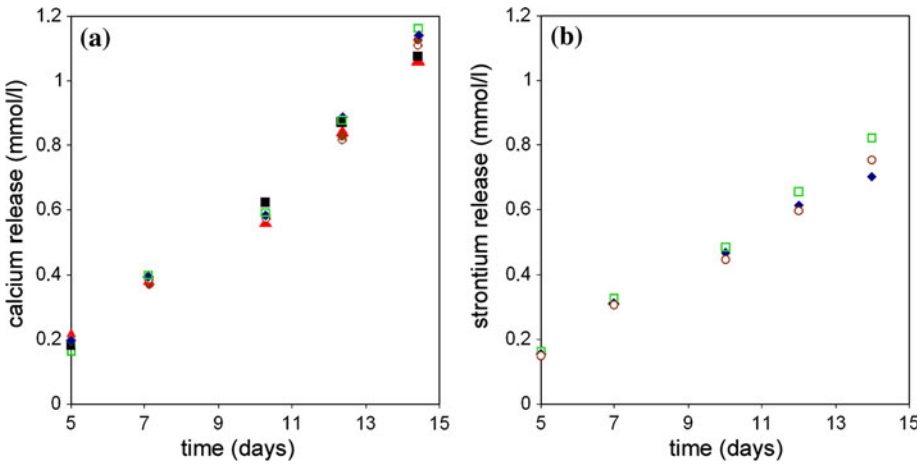

Fig. 4 Calcium (**a**) and Strontium (**b**) cumulative release from HA and SrHA as a function of soaking time in DMEM solution. Ion release from HA (*filled circle*); SrHA (*open circle*); N-HA (*filled triangle*); O-HA (*filled square*); N-SrHA (*filled diamond*); O-SrHA (*open square*)

c-axis and even more along the direction perpendicular to it, in agreement with previous data [18, 23, 26, 27].

The reduction of τ_{hkl} values indicates destabilization of crystal structure by the larger Sr atom, which might be invoked to justify the significant increase in solubility with strontium content verified by solid titration of SrHA [28].

The rate and amount of ion release can affect cells response. Therefore, we investigated Ca and Sr release from SrHA and HA in physiological solution. The analysis was carried out on disk-shaped samples, as those utilized for cell experiments, under dynamic conditions. The cumulative ion release is reported in Fig. 2 as a function of time up to 14 days. The standard deviations are smaller than the symbols. Ca release from HA is about 2 mmol/l after 3 days in physiological solution and it increases up to 4.5 mmol/l at 14 days. These quantities are almost double as much as the amounts of Ca released from SrHA after the same periods of time. Nonetheless, the sum of Sr and Ca released from SrHA is always greater than the extent of Ca release from HA, in agreement with the greater solubility of Sr-substituted HA [28]. Sr release is about 0.51% of the initial amount after 3 days, and it increases up to about 1.26% after 14 days. These values are consistent with those previously reported for Sr release from SrHA granulates of similar composition in Hanks' balanced synthetic fluid [29].

The presence of Sr can be detected by means of EDS analysis (Fig. 3a). In particular, no variation in the Sr/Ca ratio is appreciable after the release experiment. Figure 3b,

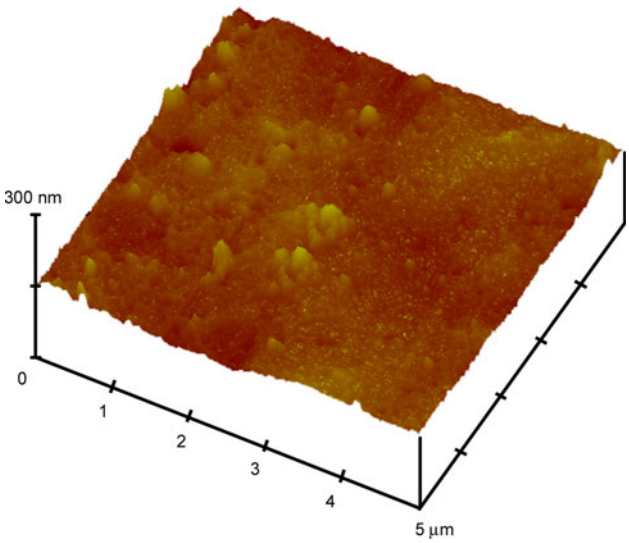

Fig. 5 AFM image of the surface of a SrHA disk-shaped sample

c reports the EDS maps of the SrHA disks before and after immersion in physiological solution. Both the maps are consistent with a homogeneous Sr distribution on the surface of the disk-shaped samples. Although the data provided by the EDS maps about the relative amounts of the two ions are to be considered qualitative, they do not give any indication of a preferential release of Sr in solution, as it would have been expected on the basis of the cumulative release data. It can be suggested that the dissolution process responsible of ionic release during immersion in NaCl solution is accompanied by a preferential precipitation of the more stable HA, which reduces Ca concentration in solution.

Osteoblast cultures were carried out in DMEM. Therefore, Sr and Ca release in DMEM was determined up to 14 days in the absence, as well as in the presence of cells. The results are reported in Fig. 4a, b for Ca and Sr, respectively. The standard deviations are smaller than the symbols. Both Sr and Ca cumulative release increase with time. However, the values are always lower than those measured in physiological solution. In particular, Sr cumulative release at 14 days assumes a mean value of

Table 2 Normal (N-OB) and Osteopenic (O-OB) osteoblasts control values at 3, 7 and 14 days of culture

Test	N-OB			O-OB		
	3 days	7 days	14 days	3 days	7 days	14 days
WST1	0.791[a] ± 0.013	1.383[a] ± 0.011	1.649[b] ± 0.016	0.576 ± 0.029	1.115 ± 0.009	1.620 ± 0.012
BAP		8.67 ± 1.77	1.92 ± 0.14		7.85 ± 0.69	1.26 ± 0.30
PC I		19.50 ± 3.03	33.72 ± 3.67		16.24 ± 4.03	23.11 ± 1.21
OC		0.42 ± 0.12	1.18 ± 0.16		0.34 ± 0.03	1.22 ± 0.09
IL-6		10.83 ± 2.53	11.86 ± 2.40		23.95[c] ± 2.42	11.17 ± 2.76
TNF-α		6.47 ± 0.04	6.77 ± 0.04		6.26 ± 0.09	6.89 ± 0.10

Statistical analysis

[a] 3 and 7 days: control cultures of normal bone derived osteoblasts (N-OB) versus osteoporotic bone derived osteoblasts (O-OB), $P < 0.0001$

[b] 14 days: N-OB versus O-OB, $P < 0.05$

[c] 7 days: N-OB versus O-OB, $P < 0.05$

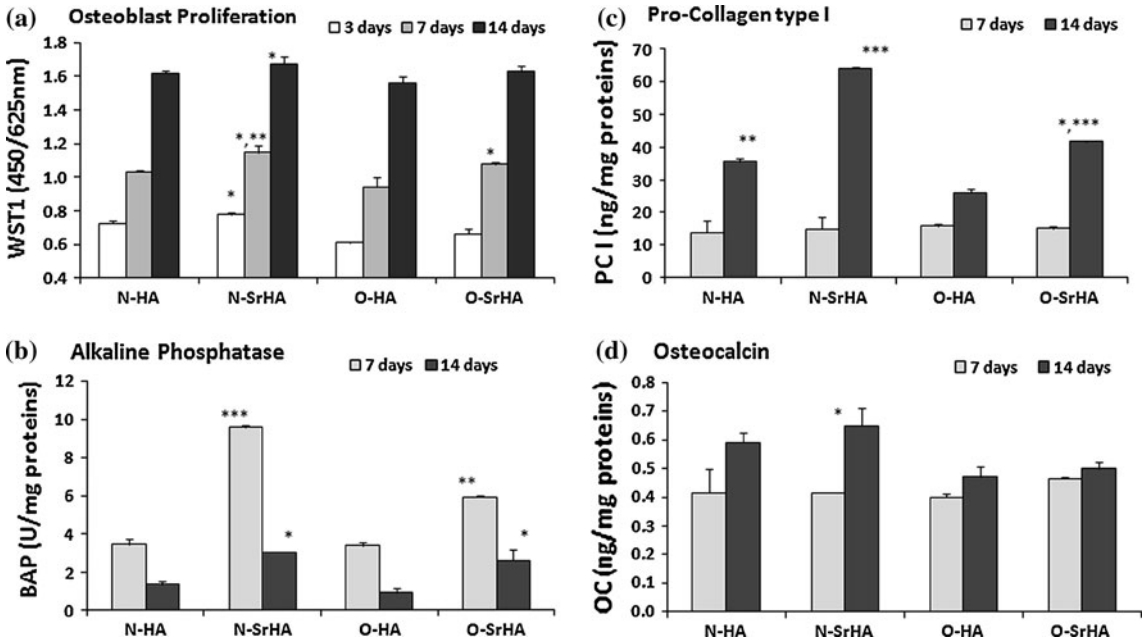

Fig. 6 Proliferation (WST1, **a**), differentiation and synthetic activity (BAP, **b**; PC I, **c**; OC, **d**) of N-OB and O-OB after 3, 7, and 14 days of culture with HA (N-HA and O-HA) and SrHA (N-SrHA and O-SrHA). Mean ± SD of six samples in triplicate. (*$P < 0.05$; **$P < 0.005$; ***$P < 0.0001$). **a** 3 days: *N-SrHA versus O-HA; 7 days: *,**N-SrHA versus N-HA, O-HA; *O-SrHA versus O-HA; 14 days: *N-SrHA versus O-HA. **b** 7 days: ***N-SrHA versus N-HA, O-HA, O-SrHA; **O-SrHA versus N-HA, O-HA; 14 days: *N-SrHA versus N-HA, O-HA; *O-SrHA versus O-HA. **c** 14 days: **N-HA versus O-HA; ***N-SrHA versus N-HA, O-HA, O-SrHA; *,***O-SrHA versus N-HA, O-HA. **d** 14 days: *N-SrHA versus O-HA

0.75 mmol/l, which corresponds to about 0.26% of the initial amount. The reduced ionic release in DMEM is justified by its ionic composition (DMEM contains 60 mg/l of Ca^{2+}, that is 1.5 mmol/l), as well as a variety of different ions and macromolecules, which remarkably decreases the solubility of HA and SrHA. In agreement with the main role of DMEM composition, the data indicate that the presence of cells does not influence the cumulative ionic release.

Cells response is greatly influenced by the roughness of the materials. Thus, we investigated the surface of the disk-shaped samples through AFM analysis. The surfaces are quite smooth, and the roughness parameters, Ra, Rq and Rmax, are quite similar for the disks of HA and SrHA with mean values of Ra = 17.55 ± 2 nm, Rq = 23.59 ± 3 nm, and Rmax = 206.07 ± 20 nm. A typical AFM image is shown in Fig. 5.

3.1 Osteoblast proliferation, activity and differentiation

The characterization of control cultures of normal and osteopenic bone derived osteoblast (Table 2) showed a significant lower proliferation of O-OB at all experimental times when compared to N-OB.

BAP and PC I production in O-OB were lower than in N-OB cultures at both 7 and 14 days, even if the differences did not reach significant values. No differences were found for OC and TNF-α values. As observed in other studies [30, 31], O-OB did not show in vitro a significant altered metabolism when compared to N-OB, except for cell proliferation rate, at all experimental times. As a matter of fact, age-related or menopause-related osteoporosis leads to loss of bone mass because of either excessive osteoclastic bone resorption or reduced osteoblastic bone formation due to decreased recruitment of osteoblasts and increased osteoclastic activity, related to impaired bone remodeling [32]. At variance, the evaluation of IL-6 showed an over-expression of IL-6 at 7 days in O-OB when compared to N-OB. At 7 days, O-OB expression of IL-6 is twice as much as that found for N-OB, in agreement with the relationship between serum IL-6 and osteoporotic bone in early postmenopausal phase [33, 34].

The results of in vitro investigation carried out on HA and SrHA indicated that the cell behaviors were greatly influenced by material composition. Results of N-OB and O-OB cultured on HA and SrHA are reported in Fig. 6. Cell proliferation was assessed at 3, 7 and 14 days by WST1 test. The results reported in Fig. 6a indicated that the cells grown on SrHA displayed higher proliferation rate than those grown on HA. In particular, N-SrHA osteoblasts showed significant higher proliferation rate at all experimental times of culture, when compared to O-HA and N-HA, whereas O-SrHA showed a significant higher proliferation at 7 days.

BAP, PC I and OC were chosen to evaluate normal and osteopenic osteoblast activation and differentiation. BAP activity is an early marker of osteoblast differentiation, and its increased expression is associated to the progressive differentiation of cultured osteoblasts [35, 36]. Subsequently type I collagen is produced, as one of the major component to form the extracellular matrix [37–39]. Collagen deposition is accompanied by an increase of OC, marker of late osteoblast differentiation [38, 40].

The results reported in Fig. 6b–d indicate that all the chosen markers were positively influenced by the addition of Sr to HA. BAP level (Fig. 6b) was significantly higher in N-SrHA and O-SrHA both at 7 and 14 days when compared to N-HA and O-HA groups. PC I production (Fig. 6c) displayed no differences at 7 days, whereas at 14 days the levels of both N-SrHA and O-SrHA groups were significantly higher than those found for N-HA and O-HA. The influence of the presence of Sr on OC (Fig. 6d) was less marked, and only the N-SrHA value reached a significant higher level at 14 days. The comparison of the data obtained on the different differentiation markers

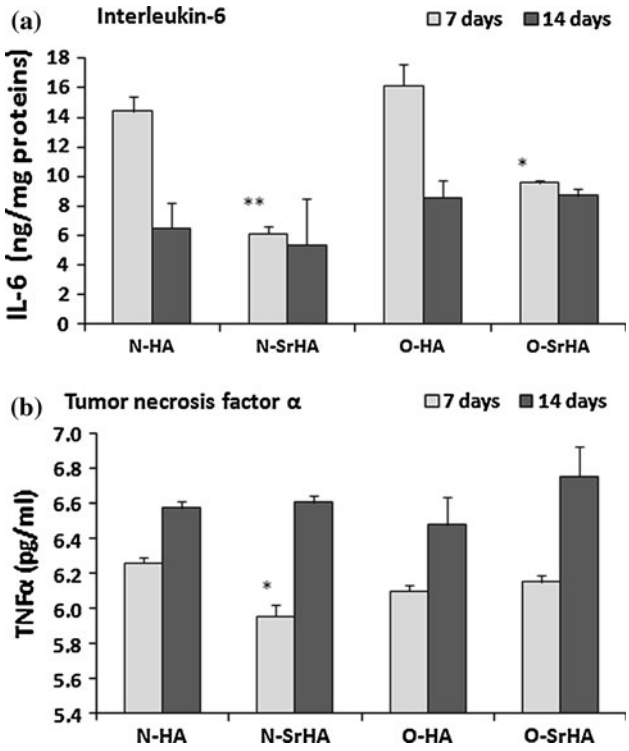

Fig. 7 Interleukin 6 (**a**), and Tumor Necrosis Factor α (**b**) of osteoblast after 14 days of culture on samples of N-OB and O-OB grown on HA (N-HA, O-HA), and on SrHA (N-SrHA, O-SrHA). Mean ± SD of six samples in triplicate. (*$P < 0.05$; **$P < 0.005$; ***$P < 0.0001$). **a** 7 days: **N-SrHA versus N-HA, O-HA; *O-SrHA versus N-HA, O-HA; **b** 7 days: *N-SrHA versus N-HA

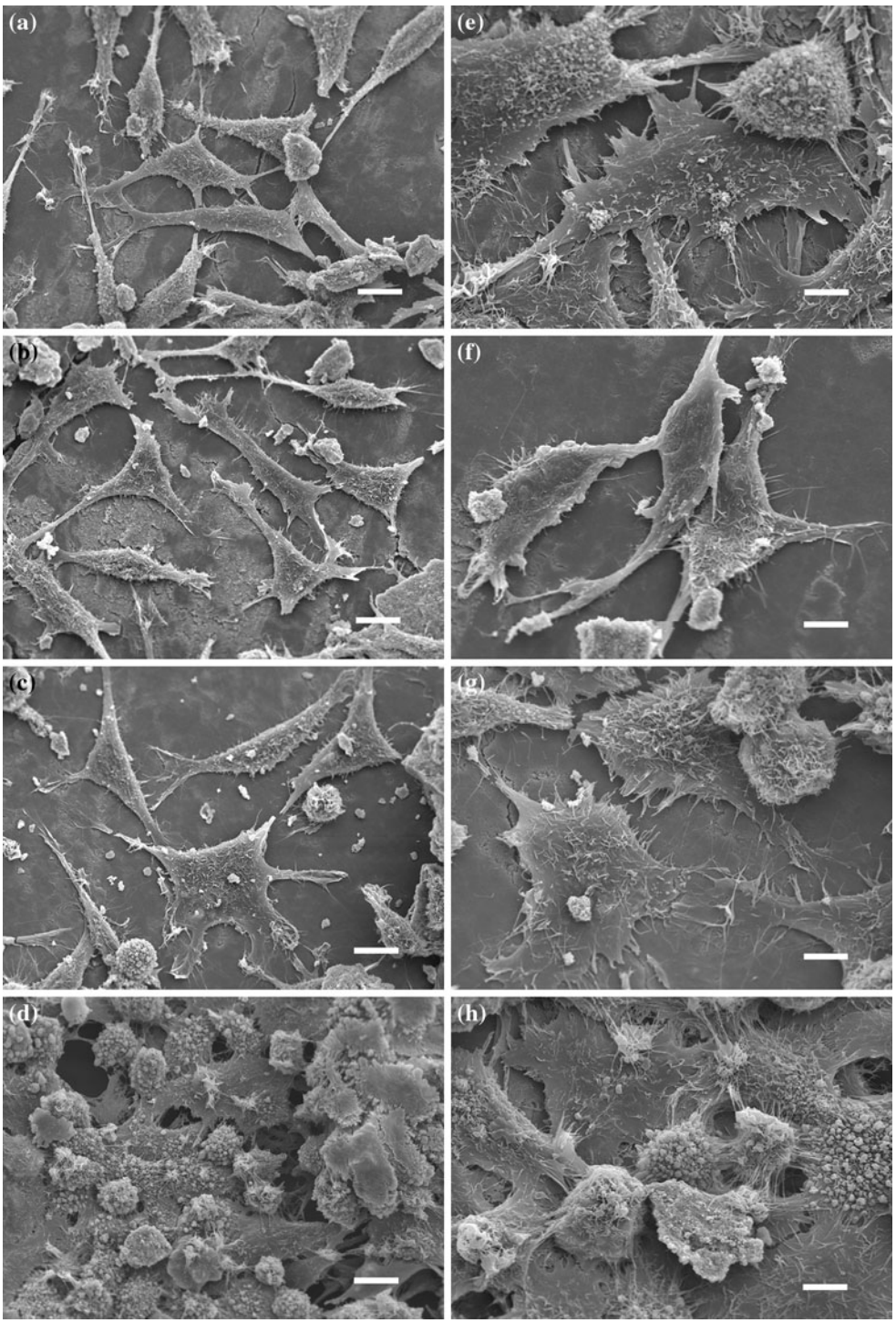

Fig. 8 SEM images of normal osteoblasts (N-OB) grown on HA (**a**, **e**) and on SrHA (**c**, **g**), and of osteopenic osteoblasts (O-OB) grown on HA (**b**, **f**) and on SrHA (**d**, **h**) for 14 days. *Scale bars* (**a**–**d**) 10 μm; *scale bars* (**e**–**h**) 5 μm

suggests that the differentiation state of the cells grown on the different materials for 14 days follows the order: N-SrHA > O-SrHA > N-HA > O-HA.

IL-6 and TNF-α were chosen as indicative for pro-inflammatory cytokine and growth factor. In fact, IL-6 has a major role in the mediation of the inflammatory and immune responses initiated by infections or injuries. Moreover, an increase of its level is related to an osteopenic state of bone tissue [41]. IL-6 has a key negative role in osteoporosis and other bone diseases, influencing

both osteoblast and osteoclast activities. It is reported that IL-6 has an inhibitory effect on bone formation and marker expression in vitro and it can stimulate osteoclasts differentiation [42, 43]. TNF-α is a pleiotropic cytokine that plays a key role in both inflammation and apoptosis [44]. The results reported in Fig. 7 show that at 7 days IL-6 (Fig. 7a) was significantly lower in N-SrHA and O-SrHA groups, and TNF-α (Fig. 7b) showed significant lower value in N-SrHA. At 14 days there were no differences among groups. These results suggest an initial down-regulatory effect of strontium upon osteoblasts production of both IL-6 and TNF-α, in good agreement with the significant reduction of their levels.

It has to be highlighted that the presence of Sr significantly decreased the level of IL-6 in N-OB and O-OB and most importantly significantly counteracted the increase of IL-6 that was observed in O-OB. These data are of special interest because Sr has an anabolic effect on bone remodeling and an inhibitory effect on osteoclast differentiation and activity that seem to be mediated by an increase in osteoprotegerin and a decrease in RANKL [7]. IL-6 secreted by osteoblasts is reported to be interrelated with the RANK/RANKL/OPG mechanism of bone resorption [45].

SEM images of the cells grown on the different materials at 14 days showed good attachment and spreading (Fig. 8). N-OB (Fig. 8a, e) grown on HA display more lamellipodia and filopodia extensions than osteopenic osteoblasts (Fig. 8b, f). Both kind of cells display even more extensions when grown on SrHA (Fig. 8c, g, d, h). Moreover, the amount of O-OB grown on the surface of SrHA disk appear particularly great (Fig. 8d, h), even if the proliferation data do not show significant differences at 14 days.

The results obtained are consistent with previous studies reporting that Sr stimulates cell proliferation, collagen synthesis, osteocalcin and alkaline phosphatase expression, and mineralization rate [10, 46]. Moreover, they confirm that the ion exerts its beneficial effect even when incorporated into HA structure [14, 15, 17, 18], and allow to state that the different results obtained on SrHA and HA are indeed due to the presence of Sr and not to other factors, such as solubility and roughness.

The data obtained on O-OB are of peculiar importance since they indicate increased levels of proliferation, alkaline phosphatase, and collagen type I, and down-regulation of IL-6 of O-OB when grown on SrHA.

4 Conclusions

The results of this work indicate that although SrHA displays a greater solubility than HA in physiological solution, calcium release in the medium utilized for cells culture (DMEM) is remarkably reduced and almost the same for the two materials. Both Sr and Ca releases are not affected by the presence and/or the different type of cells. On this basis, and in view of the same roughness of the disk-shaped samples of SrHA and HA where the cells were grown on, the different cell responses to the two materials can be ascribed to the influence of Sr. The data showed that partial substitution of Sr for Ca in HA promotes osteoblast differentiation and IL-6 down-regulation both in normal and osteopenic cells, suggesting that SrHA could be successfully employed for the preparation of biomaterials for bone tissue repair not only in normal but also in pathological conditions such as osteoporosis.

Acknowledgments This research was carried out with the financial support of MIUR.

References

1. Dimitrious R, Babis GC. Biomaterial osseointegration enhancement with biophysical stimulation. J Musculoskelet Neuronal Interact. 2007;7:253–65.
2. Lind M, Bunger C. Factors stimulating bone formation. Eur Spine J. 2001;10:S102–9.
3. Calvo-Fernandez T, Parra J, Fernandez-Gutierrez M, Vasquez-Lasa B, Lopez-Bravo A, Collia F, Perez de la Cruz MA, San Roman J. Biocompatbility of alendronate-loaded acrylic cement for vertebroplasty. Eur Cells Mater. 2010;20:260–73.
4. Marie PJ. Strontium ranelate: a novel mode of action optimizing bone formation and resorption. Osteoporos Int. 2005;16:S7–10.
5. Ammann P. Strontium ranelate: a novel mode of action leading to renewed bone quality. Osteoporos Int. 2005;16:S11–5.
6. Deeks ED, Dhillon S. Strontium ranelate: a review of its use in the treatment of postmenopausal osteoporosis. Drugs. 2010;70:733–59.
7. Gallacher SJ, Dixon T. Impact of treatments for postmenopausal osteoporosis (biphosphonates, parathyroid hormone, strontium ranelate and denosumab) on bone quality: a systematic review. Calcif Tissue Int. 2010;87:469–84.
8. Dahl SG, Allain P, Marie PJ, Mauras Y, Boivin G, Ammann P, Tsouderos Y, Delmas PD, Christiansen C. Incorporation and distribution of strontium in bone. Bone. 2001;28:446–53.
9. Marie PJ, Ammann P, Boivin G, Rey C. Mechanisms of action and therapeutic potential of strontium in bone. Calcif Tissue Int. 2001;69:121–9.
10. Bonnelye E, Chabadel A, Saltel F, Jurdic P. Dual effect of strontium ranelate: stimulation of osteoblast differentiation and inhibition of osteoclast formation and resorption in vitro. Bone. 2008;42:129–38.
11. Marie PJ, Hott M, Modrowski D, Depollak C, Guillemain J, Deloffre P, Tsouderos P. An uncoupling agent containing strontium prevents bone loss by depressing bone-resorption and maintaining bone-formation in estrogen-deficient rats. J Bone Miner Res. 1993;8:607–15.
12. Reginster JY, Bruyère O, Sawicki A, Roces-Varela A, Fardellone P, Roberts A, Devogelaer JP. Long-term treatment of postmenopausal osteoporosis with strontium ranelate: results at 8 years. Bone. 2009;45:1059–64.
13. Xue W, Hosick HL, Bandyopadhyay A, Bose S, Ding C, Luk KDK, Cheung KMC, Lu WW. Preparation and cell-materials interactions of plasma sprayed strontium-containing hydroxyapatite coating. Surf Coat Technol. 2007;201:4685–93.

14. Capuccini C, Torricelli P, Sima F, Boanini E, Ristoscu C, Bracci B, Socol G, Fini M, Mihailescu IN, Bigi A. Strontium-substituted hydroxyapatite coatings synthesized by pulsed-laser deposition: in vitro osteoblast and osteoclast response. Acta Biomater. 2008;4:1885–93.
15. Gentleman E, Fredholm YC, Jell G, Lotfibakhshaiesh N, O'Donnell MD, Hill RG, Stevens MM. The effects of strontium-substituted bioactive glasses on osteoblasts and osteoclasts in vitro. Biomaterials. 2010;31:3949–56.
16. Isaac J, Nohra J, Lao J, Jallot E, Nedelec JM, Berdal A, Sautier JM. Effects of strontium-doped bioactive glass on the differentiation of cultured osteogenic cells. Eur Cells Mater. 2011;21: 130–43.
17. Boanini E, Gazzano M, Bigi A. Ionic substitutions in calcium phosphates synthesized at low temperature. Acta Biomater. 2010;6:1882–94.
18. Capuccini C, Torricelli P, Boanini E, Gazzano M, Giardino R, Bigi A. Interaction of Sr-doped hydroxyapatite nanocrystals with osteoclast and osteoblast-like cells. J Biomed Mater Res. 2009;89A:594–600.
19. Zhang H, Lewis CG, Aronow MS, Gronowicz GA. The effects of patient age on human osteoblast' response to Ti-6Al-4 V implants in vitro. J Orthop Res. 2004;22:30–8.
20. Fini M, Giavaresi G, Torricelli P, Krajewski A, Ravaglioli A, Belmonte MM, Biagini G, Giardino R. Biocompatibility and osseintegration in osteoporotic bone. A preliminary in vitro and in vivo study. J Bone and Joint Surg (Br). 2001;1(83B):139–43.
21. Torricelli P, Fini M, Rocca M, Giavaresi G, Giardino R. In vitro pathological model of osteopenia to test orthopaedic biomaterials. Art Cells Blood Subst Immobil Biotechnol. 2000;28:181–92.
22. Fini M, Giavaresi G, Nicoli Aldini N, Torricelli P, Morrone G, Guzzardella GA, Giardino R, Krajewski A, Ravaglioli A, Mattioli Belmonte M, De Benedittis A, Biagini G. The effect of osteopenia on the osteointegration of different biomaterials: histomorphometric study in rats. J Mater Sci: Mater Med. 2000;11: 579–85.
23. Bigi A, Boanini E, Capuccini C, Gazzano M. Strontium-substituted hydroxyapatite nanocrystals. Inorg Chim Acta. 2007;360: 1009–16.
24. Giavaresi G, Fini M, Gnudi S, De Terlizzi F, Carpi A, Giardino R. The femoral distal epiphysis of ovariectomized rats as a site for studies on osteoporosis: structural and mechanical evaluations. Clin Exp Rheumatol. 2002;20:171–8.
25. Klug HP, Alexander LE. X-ray diffraction procedures for polycrystalline and amorphous materials. New York: Wiley-Interscience; 1974.
26. Terra J, Rodrigues Dourado E, Eon JG, Ellis DE, Gonzalez G, Malta Rossi A. The structure of strontium-doped hydroxyapatite: an experimental and theoretical study. Phys Chem Chem Phys. 2009;11:568–77.
27. O'Donnell MD, Fredholm Y, de Rouffignac A, Hill RG. Structural analysis of a series of strontium-substituted apatites. Acta Biomater. 2008;4:1455–64.
28. Pan HB, Li ZY, Lam WM, Wong JC, Darvell BW, Luk KDK, Lu WW. Solubility of strontium-substituted apatite by solid titration. Acta Biomater. 2009;5:1678–85.
29. Landi E, Sprio S, Sandri M, Celotti G, Tampieri A. Development of Sr and CO3 co-substituted hydroxyapatites for biomedical applications. Acta Biomater. 2008;4:656–63.
30. Torricelli P, Fini M, Giavaresi G, Giardino R. Osteoblasts cultured from osteoporotic bone: a comparative investigation on human and animal-derived cells. Art Cells Blood Subs Immob Biotech. 2003;31(3):263–77.
31. Bigi A, Panzavolta S, Sturba L, Torricelli P, Fini M, Giardino R. Normal and osteopenic bone derived osteoblast response to a biomimetic gelatin–calcium phosphate bone cement. J Biomed Mater Res. 2006;78A:739–45.
32. Marie PJ. Cellular and molecular alterations of osteoblasts in human disorders of bone formation. Histol Histopathol. 1999;14:525–38.
33. Scheidt-Nave C, Bismar H, Leidig-Bruckner G, Woitge H, Seibel MJ, Ziegler R, Pfeilschifter J. Serum interleukin 6 is a major predictor of bone loss in women specific to the first decade past menopause. J Clin Endocrinol Metab. 2001;86:2032–42.
34. Pino AM, Rıos S, Astudillo P, Fernandez M, Figueroa P, Seitz G, Rodrıguez JP. Concentration of adipogenic and proinflammatory cytokines in the bone marrow supernatant fluid of osteoporotic women. J Bone Miner Res. 2010;25:492–8.
35. Malaval L, Liu F, Roche P, Aubin JE. Kinetics of osteoprogenitor proliferation and osteoblast differentiation in vitro. J Cell Biochem. 1999;74:616–27.
36. Atsushi E, Korenori O, Satoshi I, Shigeyuki E, Takayoshi N, Yukichi U. Effects of α-TCP and TetCP on MC3T3–E1 proliferation, differentiation and mineralization. Biomaterials. 2003; 24:831–6.
37. Franceschi RT, Iyer BS. Relationship between collagen synthesis and expression of the osteoblast phenotype in MC3T3–E1 cells. J Bone Miner Res. 1992;7:235–46.
38. Cowles EA, DeRome D, Pastizzo G, Brailey LL, Gronowicz GA. Mineralization and the expression of matrix proteins during in vivo bone development. Calcif Tissue Int. 1998;62:74–82.
39. Fini M, Giardino R, Borsari V, Torricelli P, Rimondini L, Giavaresi G, Nicoli Aldini N. In vitro behaviour of osteoblasts cultured on orthopaedic biomaterials with different surface roughness, uncoated and fluorohydroxyapatite-coated, relative to the in vivo osteointegration rate. Int J Artif Organs. 2003;26: 520–8.
40. Mayr-Wohlfart U, Fiedler J, Gunther KP, Puhl W, Kessler S. Proliferation and differentiation rates of a human osteoblast-like cell line (SaOS-2) in contact with different bone substitute materials. J Biomed Mater Res. 2001;57:132–9.
41. Kishimoto T, Akira S, Taga T. Interleukin-6 and its receptor: a paradigm for cytokines. Science. 1992;258(5082):593–7.
42. Axmann R, Böhm C, Krönke G, Zwerina J, Smolen J, Schett G. Inhibition of interleukin-6 receptor directly blocks osteoclast formation in vitro and in vivo. Arthritis Rheum. 2009;60(9):2747–56.
43. Blanchard F, Duplomb L, Baud'hium M, Brounais B. The dual role of IL-6type cytokines on bone remodeling and bone tumors. Cytokine Growth Factor Rev. 2009;20:19–28.
44. MacEwan DJ. TNF ligands and receptors: a matter of life and death. Br J Pharmacol. 2002;135:855–75.
45. Steeve KT, Marc P, Sandrine T, Dominique H, Yannick F. IL-6, RANKL, TNF-alpha/IL-1: interrelations in bone resorption pathophysiology. Cytokine Growth Factor Rev. 2004;15:49–60.
46. Atkins GJ, Welldon KJ, Halbout P, Findlay DM. Strontium ranelate treatment of human primary osteoblasts promotes an osteocyte-like phenotype while eliciting an osteoprotegerin response. Osteoporos Int. 2009;20:653–64.